

RESEARCH ARTICLE

STEM CELLS AND REGENERATION

DNMT3L promotes quiescence in postnatal spermatogonial progenitor cells

Hung-Fu Liao^{1,2}, Wendy S. C. Chen^{1,3}, Yu-Hsiang Chen¹, Tzu-Hao Kao¹, Yen-Tzu Tseng¹, Chien-Yueh Lee⁴, Yu-Chiao Chiu⁴, Pei-Lung Lee¹, Qian-Jia Lin^{5,6}, Yung-Hao Ching⁷, Kenichiro Hata⁸, Winston T. K. Cheng⁹, Mong-Hsun Tsai¹, Hiroyuki Sasaki¹⁰, Hong-Nerng Ho¹¹, Shinn-Chih Wu³, Yen-Hua Huang^{5,6}, Pauline Yen² and Shau-Ping Lin^{1,12,13,14,*}

ABSTRACT

The ability of adult stem cells to reside in a quiescent state is crucial for preventing premature exhaustion of the stem cell pool. However, the intrinsic epigenetic factors that regulate spermatogonial stem cell quiescence are largely unknown. Here, we investigate in mice how DNA methyltransferase 3-like (DNMT3L), an epigenetic regulator important for interpreting chromatin context and facilitating *de novo* DNA methylation, sustains the long-term male germ cell pool. We demonstrated that stem cell-enriched THY1⁺ spermatogonial stem/progenitor cells (SPCs) constituted a DNMT3L-expressing population in postnatal testes. DNMT3L influenced the stability of promyelocytic leukemia zinc finger (PLZF), potentially by downregulating *Cdk2/CDK2* expression, which sequestered CDK2-mediated PLZF degradation. Reduced PLZF in *Dnmt3l* KO THY1⁺ cells released its antagonist, Sal-like protein 4A (SALL4A), which is associated with overactivated ERK and AKT signaling cascades. Furthermore, DNMT3L was required to suppress the cell proliferation-promoting factor SALL4B in THY1⁺ SPCs and to prevent premature stem cell exhaustion. Our results indicate that DNMT3L is required to delicately balance the cycling and quiescence of SPCs. These findings reveal a novel role for DNMT3L in modulating postnatal SPC cell fate decisions.

KEY WORDS: DNMT3L, Proliferation, Spermatogonial progenitor cell, Quiescence, Mouse

INTRODUCTION

Stem cells are crucial for tissue homeostasis and regeneration (Orford and Scadden, 2008; Cheung and Rando, 2013). Spermatogenesis is

a well-characterized stem cell-dependent process. Spermatogonial stem cells reside in a subpopulation of mouse male germ cells, spermatogonial stem/progenitor cells (SPCs), which include A_{paired} (A_{pr}) and A_{aligned} (A_{al}) spermatogonia (Nakagawa et al., 2007, 2010). SPCs provide the fundamental source of cells for spermatogenesis and are responsible for the spermatogenic cycle throughout the reproductive lifespan of males. These cells can produce differentiating spermatogonia, which undergo a series of divisions to mature into differentiated spermatogonia and spermatocytes, ultimately developing into functional spermatozoa (Oatley and Brinster, 2012).

An adequate number of stem cells remain in a relatively quiescent state to avoid premature exhaustion and to allow long-term maintenance of a functional stem cell population (Ema and Suda, 2012; Cheung and Rando, 2013). Cyclin-dependent kinase 2 (CDK2), a positive regulator of cell cycle progression, has been suggested as a regulator of the quiescence-proliferation decision in various somatic cells (Spencer et al., 2013) and functions in promyelocytic leukemia zinc finger (PLZF) stability by mediating PLZF phosphorylation, rendering it prone to ubiquitylation and subsequent degradation (Costoya et al., 2008). PLZF and Sal-like protein 4 (SALL4) are crucial regulators of cell quiescence and proliferation (Yang et al., 2008b; Hobbs et al., 2012). PLZF has been characterized as a DNA-binding transcriptional repressor of cell cycle progression, whereas SALL4 is an oncogene due to its cell growth-stimulating properties. It participates in the modulation of several signal transduction cascades, including the MAPK kinase/ERK-ERK (MEK-ERK) and AKT pathways (Yeyati et al., 1999; McConnell et al., 2003; Yang et al., 2008a; Rice et al., 2009; Aguila et al., 2011). PLZF and SALL4 are SPC-specific molecules expressed in mouse testes (Gassei and Orwig, 2013). PLZF antagonizes SALL4A activity and prevents SPC cycling; however, an increase in the SALL4-to-PLZF ratio promotes SPC differentiation (Hobbs et al., 2012).

DNMT3L is an epigenetic modifier closely associated with transcriptional repression and is crucial for genome-wide reprogramming in quiescent embryonic germ cells (Aapola et al., 2000, 2001; Bourc'his et al., 2001; Buas et al., 2004). DNMT3L itself does not possess enzymatic activity but acts as a processive catalyst and cooperates with other DNA methyltransferases (DNMTs) via its C-terminus to promote the *de novo* methylation of DNA sequences, including retrotransposons, gene bodies and the regulatory sequences of imprinted genes (Bourc'his et al., 2001; Chedin et al., 2002; Hata et al., 2002; Bourc'his and Bestor, 2004; Suetake et al., 2004; Kato et al., 2007; Holz-Schietinger and Reich, 2010; Niles et al., 2011; Smallwood et al., 2011; Van Emburgh and Robertson, 2011; Arand et al., 2012; Kobayashi et al., 2012; Ichyanagi et al., 2013). In addition, DNMT3L contains a plant homeodomain (PHD)-like domain that can recruit histone

¹Institute of Biotechnology, National Taiwan University, Taipei 106, Taiwan. ²Institute of Biomedical Sciences, Academia Sinica, Taipei 115, Taiwan. ³Department of Animal Science and Technology, National Taiwan University, Taipei, Taiwan. ⁴Graduate Institute of Biomedical Electronics and Bioinformatics, National Taiwan University, Taipei 106, Taiwan. ⁵Department of Biochemistry, Graduate Institute of Medical Sciences, College of Medicine, Taipei Medical University Hospital, Taipei Medical University, Taipei 110, Taiwan. ⁶Center for Reproductive Medicine, Taipei Medical University Hospital, Taipei Medical University, Taipei 110, Taiwan. ⁷Department of Molecular Biology and Human Genetics, Tzu Chi University, Hualien 97004, Taiwan. ⁸Department of Maternal-Fetal Biology, National Research Institute for Child Health and Development, Okura, Setagaya, Tokyo 157-8535, Japan. ⁹Department of Animal Science and Biotechnology, Tunghai University, Taichung 40704, Taiwan. ¹⁰Department of Molecular Genetics, Medical Institute of Bioregulation, Kyushu University, Fukuoka 812-8582, Japan. ¹¹Department of Obstetrics and Gynecology, College of Medicine and the Hospital, National Taiwan University, Taipei 100, Taiwan. ¹²Agricultural Biotechnology Research Center, Academia Sinica, Taipei 115, Taiwan. ¹³Center for Systems Biology, National Taiwan University, Taipei 106, Taiwan. ¹⁴Research Center for Developmental Biology and Regenerative Medicine, National Taiwan University, Taipei 106, Taiwan.

*Author for correspondence (shaupinglin@ntu.edu.tw)

This is an Open Access article distributed under the terms of the Creative Commons Attribution License (<http://creativecommons.org/licenses/by/3.0>), which permits unrestricted use, distribution and reproduction in any medium provided that the original work is properly attributed.

modifiers, such as histone deacetylase 1 (HDAC1), or bind to the N-terminus of histone H3 when the lysine 4 of histone H3 is unmethylated (Aapola et al., 2002; Deplus et al., 2002; Jia et al., 2007; Ooi et al., 2007). Moreover, DNMT3L may mediate the DNA methylation of properly chromatinized DNA templates (Wienholz et al., 2010).

Significant levels of *Dnmt3l* and DNMT3L are expressed in prospermatogonia, the precursors of SPCs, in the testes of fetal and newborn mice (Bourc'his and Bestor, 2004; Webster et al., 2005). Their expression levels decline drastically shortly after birth, and the DNMT3L protein becomes undetectable in 4–6 day postpartum (dpp) testes (Sakai et al., 2004).

Dnmt3l deficiency results in germ cell depletion in adult testes. One-week-old *Dnmt3l* knockout (KO) and littermate control (wild-type and heterozygous) testes contain similar numbers of spermatogonia (Hata et al., 2002). However, *Dnmt3l* KO male mice gradually lose their germ cells, which becomes apparent at 2 weeks of age, whereas the tubules of adults (8–10 weeks of age) contain only Sertoli cells (Hata et al., 2006; La Salle et al., 2007). A deficiency in DNMT3L accumulation causes defects in chromosome synapsis during the meiotic stage of spermatocyte development, although there is no detectable DNMT3L expression in wild-type spermatocytes (Bourc'his and Bestor, 2004; Mahadevaiah et al., 2008).

The presence of weak but detectable levels of *Dnmt3l* mRNA in postnatal testes suggests that a subpopulation of germ cells may express DNMT3L (La Salle et al., 2004; Hata et al., 2006). Thus, identifying and characterizing DNMT3L-expressing cells in postnatal germ cells would elucidate a potentially direct function of DNMT3L in postnatal male germ cells.

This study revealed that stem cell-enriched THY1⁺ SPCs in postnatal testes expressed significant levels of DNMT3L. A DNMT3L deficiency caused defects in modulating the quiescent state of THY1⁺ SPCs, resulting in stem cell over-proliferation and eventually germ cell exhaustion, indicating the pivotal role of DNMT3L in maintaining the postnatal male germ line.

RESULTS

Abnormal distribution of SPCs in *Dnmt3l* KO postnatal testes

The complete germ cell exhaustion in adult *Dnmt3l* KO testes suggests that DNMT3L may be important for SPC maintenance in postnatal testes (Bourc'his and Bestor, 2004; Webster et al., 2005; Hata et al., 2006). We examined the SPC distribution in postnatal testes using PLZF staining because PLZF is strongly expressed in all types of SPCs (Sada et al., 2009; Gassei and Orwig, 2013). Immunostaining of whole-mount dispersed seminiferous tubules from mice between 4 dpp and 4 weeks of age indicated that the *Dnmt3l* KO testes began to display an uneven distribution of PLZF⁺ cells at 7 dpp (data not shown). By 8 dpp, a clearly uneven distribution of PLZF⁺ cells was observed in the *Dnmt3l* KO testes compared with wild-type testes (Fig. 1A, top lane): some segments of seminiferous tubules contained many PLZF⁺ cells (Fig. 1A, middle lane), whereas other segments had very few PLZF⁺ cells (Fig. 1A, bottom lane). Additional immunostaining of 8 dpp testis sections confirmed the aberrant distribution of PLZF⁺ cells in *Dnmt3l* KO testes (Fig. 1B). The average number of PLZF⁺ cells per tubule cross-section in the mutant testes was not significantly different from that in wild-type testes at 8 dpp (Fig. 1C). However, while the wild-type testes indicated a bell-shaped distribution of the number of PLZF⁺ cells in each cross-section, the mutant testes followed a distorted distribution; a large proportion of the cross-sections contained either very few or many PLZF⁺ cells (Fig. 1D). Thus, the progressive loss of germ cells in *Dnmt3l* KO postnatal testes may be caused by dysregulated SPCs.

Significant expression of DNMT3L in postnatal THY1⁺ cells

To determine whether DNMT3L is expressed and functions in postnatal germline stem/progenitor cells, we used an anti-THY1 antibody with magnetic beads to isolate the stem cell-enriched population (THY1⁺ cells) from mouse testes at several postnatal stages. *Thy1* mRNA exhibited an approximate 25-fold enrichment in 8 dpp THY1⁺ cells compared with THY1⁻ cell populations (Fig. 2A). Furthermore, 98±0.9% and 98±0.5% of the THY1⁺ cell

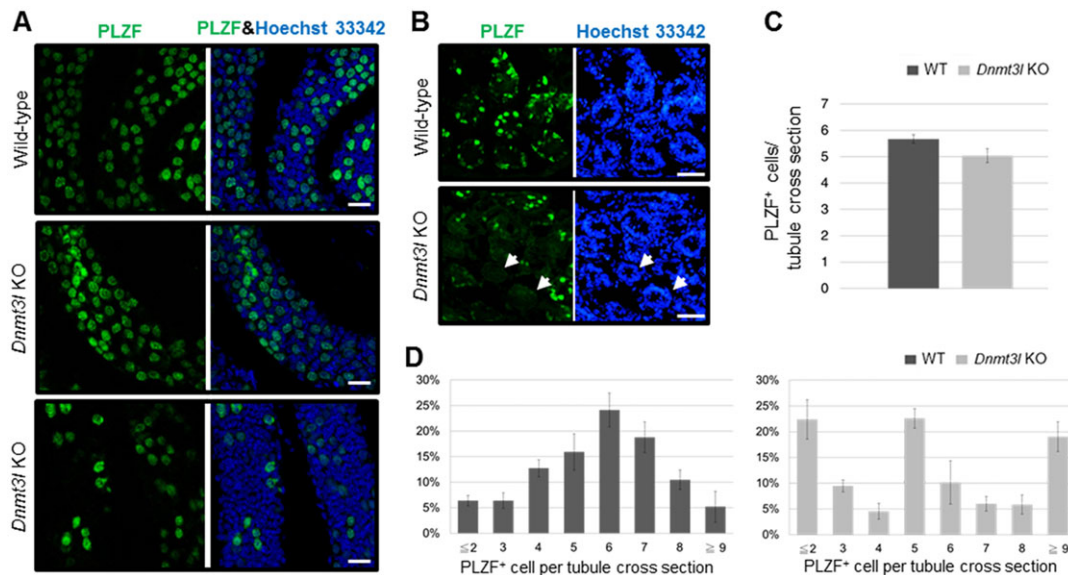


Fig. 1. Abnormal distribution of SPCs in postnatal *Dnmt3l* KO testes. (A,B) Immunostaining of 8 dpp seminiferous tubules (A) and testis sections (B) with an anti-PLZF antibody. The two frames of each panel represent the same tubule/cross-section. The arrows in B indicate cross-sections deprived of PLZF⁺ cells. Green, PLZF; blue, Hoechst 33342. Scale bars: 25 μ m. (C) Quantification of PLZF⁺ cells in 8 dpp testis sections. (D) Distribution of PLZF⁺ cells per tubule cross-section in 8 dpp wild-type and *Dnmt3l* KO testes. These results were compiled by scoring 270 randomly selected round tubules from four biological replicates. Data are mean±s.e.m.

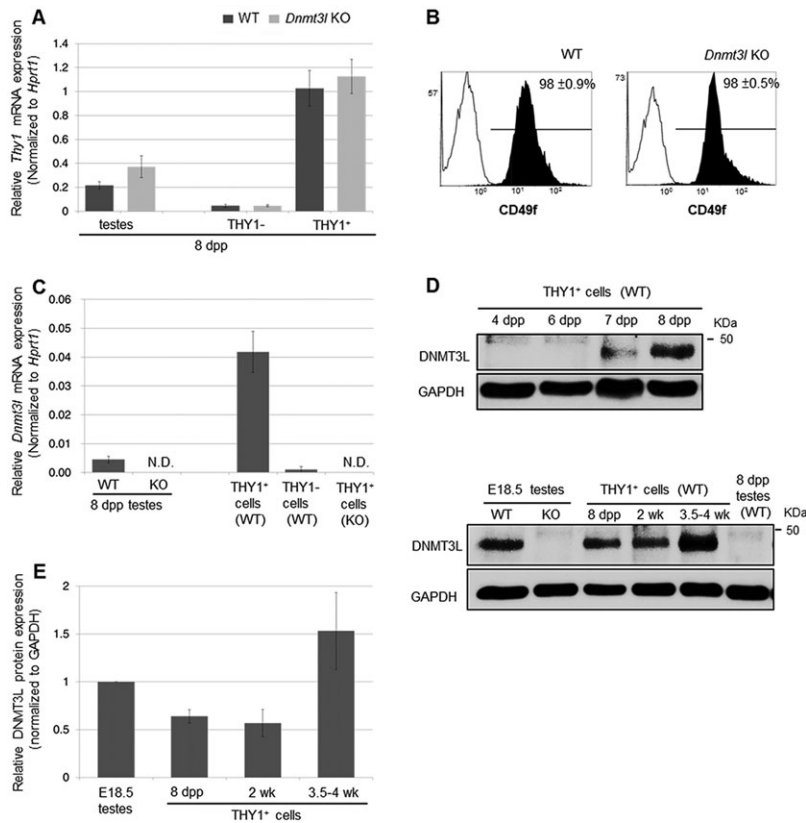


Fig. 2. Expression of DNMT3L in developing mouse testes and purified THY1⁺ germ cells. (A) Relative expression levels of *Thy1* mRNA in 8 dpp testes and in different testis cell fractions. (B) Flow cytometry analysis of isolated 8 dpp THY1⁺ cells labeled with PE-conjugated anti-CD49f antibody. The values represent the mean ± s.e.m. of at least three independent experiments. (C) Relative expression levels of *Dnmt3l* mRNA in 8 dpp testes and THY1⁺ cells. (D) Western blotting of DNMT3L expression in E18.5 testes and in postnatal THY1⁺ cells. A total of 15 µg of protein was loaded into each lane. (E) Quantitative analysis of DNMT3L expression in E18.5 testes and in THY1⁺ cells isolated from 8 dpp, 13–14 dpp, and 24–27 dpp testes. E, embryonic day; dpp, days postpartum; ND, non-detectable; WT, wild type; KO, *Dnmt3l* KO. Data in A, C and E are mean ± s.e.m. of at least three independent experiments.

populations isolated from 8 dpp wild-type and *Dnmt3l* KO testes, respectively, were positive for an SPC marker, CD49f (Fig. 2B), indicating that the isolated populations were enriched for SPCs. qPCR analyses revealed that wild-type THY1⁺ cells, but not wild-type THY1⁻ cells or *Dnmt3l* KO THY1⁺ cells, expressed a significant level of *Dnmt3l* mRNA (Fig. 2C). Furthermore, we analyzed DNMT3L expression in 4 dpp to 4-week-old wild-type THY1⁺ cells and found that THY1⁺ cells expressed significant levels of DNMT3L from 8 dpp onwards (Fig. 2D,E). Compared with entire 8 dpp testes, the isolated 8 dpp THY1⁺ cells displayed a significantly higher level of DNMT3L expression (Fig. 2D), suggesting the role of DNMT3L in SPC maintenance after birth.

Increased cell proliferation and elevated CDK2 expression in *Dnmt3l* KO THY1⁺ SPCs

At 8 dpp, the isolated THY1⁺ cells represented approximately $4.31 \pm 0.23\%$ and $6.05 \pm 0.46\%$ of the total cells in the wild-type and *Dnmt3l* KO testes, respectively. This finding was consistent with the qPCR results indicating that the *Dnmt3l* KO testes displayed a higher level of *Thy1* mRNA than the wild-type testes (Fig. 2A). To determine the proliferative potential of postnatal THY1⁺ SPCs, we performed immunostaining of Ki67, which is a protein strictly associated with cycling cells. The percentages of non-quiescent SPCs in these prepubertal *Dnmt3l* KO populations were significantly higher than those in the wild-type populations, which displayed significant DNMT3L expression (Fig. 2D and Fig. 3A, and see supplementary material Fig. S1).

We then studied the expression of cell cycling regulators, such as CDKs and cyclins, to explain the over-representation of proliferating cells among *Dnmt3l* KO THY1⁺ cells (Fig. 3B). Compared with wild-type cells, 8 dpp *Dnmt3l* KO THY1⁺ cells showed significantly increased *Cdk2* expression (Fig. 3B). Subsequent western blotting confirmed elevated CDK2 protein expression in *Dnmt3l* KO THY1⁺

cells (Fig. 3C). The mouse *Cdk2* promoter region contains two CpG islands (−188 to +63 and −677 to −536) with several binding sites for transcription factors, including SP1, AP1 and ETS1 (Fig. 3D) (Heinemeyer et al., 1998; Sun et al., 2011). The bisulfite sequencing results revealed that compared with wild-type cells, the *Dnmt3l* KO THY1⁺ cells displayed hypomethylation of the distal CpG island, particularly at a putative ETS1-binding-site (EBS) (Fig. 3D). We did not find obvious differences in the cytosine methylation of the proximal CpG island (see supplementary material Fig. S2).

To assess the importance of the distal CpG island for *Cdk2* promoter activity, CD49f⁺ GSCs were transfected with reporter plasmids containing different components of the *Cdk2* promoter and analyzed for luciferase activity. Compared with the plasmid containing both the proximal and distal CpG islands, an EBS mutation or the removal of the distal CpG island resulted in significantly decreased luciferase activity (Fig. 3E), suggesting that the EBS and the distal CpG island are important for *Cdk2* transcriptional activity. We also performed chromatin immunoprecipitation (ChIP) using an anti-ETS1 antibody. Whereas there was no significant difference in ETS1 protein expression between wild-type and *Dnmt3l* KO THY1⁺ cells (Fig. 3G), significantly increased ETS1 was bound to the DNA hypomethylated, H3K4me3-overaccumulated *Cdk2* promoter in 8 dpp *Dnmt3l* KO THY1⁺ cells (Fig. 3F). These data suggest that DNMT3L mediates CDK2 expression through transcriptional regulation and support a role for DNMT3L in influencing the cycling/quiescent fates of SPCs.

Decreased quiescence among *Dnmt3l* KO THY1⁺ SPCs

Previous studies have shown that SPCs display PLZF/H3K9me3 colocalization (Payne and Braun, 2006) and exhibit two major PLZF nuclear distribution patterns: perinuclear distribution is associated with quiescent and non-differentiated SPCs, whereas a punctate distribution pattern characterizes active/differentiating SPCs (Hobbs

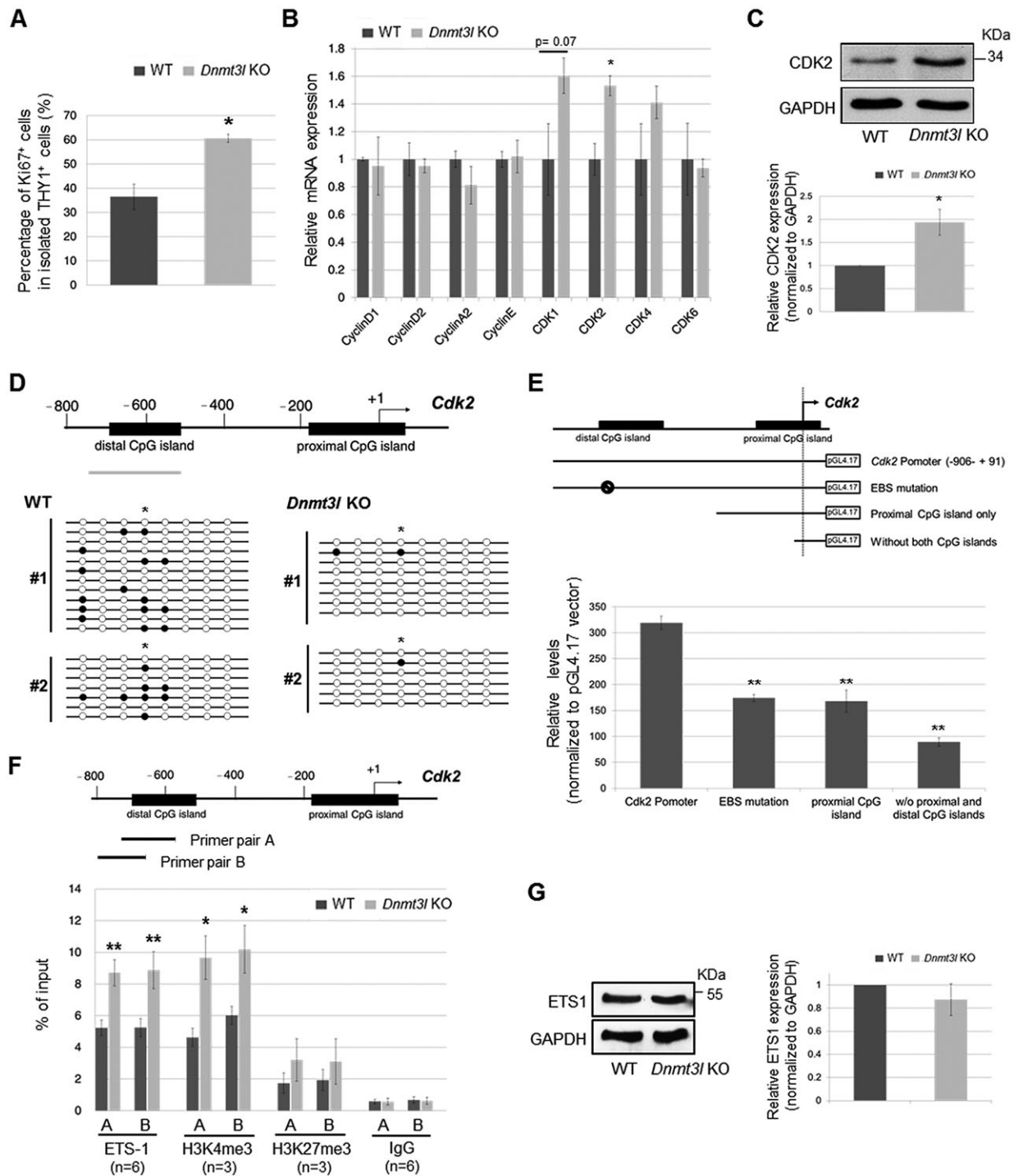


Fig. 3. Increased proliferation, *Cdk2*/CDK2 elevation and ETS1 accumulation at the *Cdk2* promoter in *Dnmt3l* KO THY1⁺ cells. (A) Percentages of Ki67⁺ cells in isolated 8 dpp THY1⁺ cells, analyzed by immunocytochemistry. Randomly selected groups of 400 cells from four independent experiments were analyzed. (B) Relative mRNA expression levels of cyclins and Cdk2 in 8 dpp THY1⁺ cells. The means and s.e.m. were calculated from three independent experiments performed in triplicate. (C) Relative CDK2 protein expression levels of 8 dpp THY1⁺ cells ($n=6$, $P=0.012$). (D) The mouse *Cdk2* promoter and the bisulfite sequencing analysis of the *Cdk2* promoter in isolated 8 dpp THY1⁺ cells. The black boxes denote CpG islands in the *Cdk2* promoter and the gray line represents the sequenced region. The batch numbers are indicated on the left. Five postnatal mice of the same genotype were used for each batch. The white and black circles indicate unmethylated CpGs and methylated CpGs, respectively. The asterisks mark putative ETS1-binding sites predicted using the TFSEARCH program. (E) Luciferase reporter assays of the mouse *Cdk2* promoter in the presence or absence of the distal CpG island. Different lengths of the *Cdk2* promoter were fused to a luciferase reporter (pGL4.17), and the luciferase activity was measured in CD49f⁺ GSCs transfected with these reporter constructs. Data are mean±s.e.m. ($n=8$) and are representative of two independent experiments. (F) Real-time PCR analysis of ChIP products. Antibodies against ETS1, H3K4me3, H3K27me3 and IgG were used to immunoprecipitate fragmented chromatin from 8 dpp THY1⁺ cells. Primer pairs A and B were used for the quantitative real-time PCR analysis and the fold enrichment was normalized to the input. Data are mean±s.e.m. (G) ETS1 expression in 8 dpp wild-type and *Dnmt3l* KO THY1⁺ cells ($n \geq 3$). n , the number of independently performed experiments; WT, wild type. Data are mean±s.e.m.; * $P < 0.05$ and ** $P < 0.01$, respectively (Student's *t*-test).

et al., 2012). Wild-type and *Dnmt3l* KO THY1⁺ cells at 8 dpp contained 98.3%±0.9% and 96.6%±1.2% PLZF⁺ cells, respectively (Fig. 4A). However, compared with their wild-type counterparts, some *Dnmt3l* KO THY1⁺ cells displayed weaker PLZF signals (Fig. 4B, arrow). In addition to punctate and perinuclear localizations, a small fraction of THY1⁺ cells displayed a diffuse PLZF/H3K9me3 staining pattern (Fig. 4C,D). These cells represented A_s and A_{pr} spermatogonia based on the germ cell arrangement in whole-mount seminiferous tubules (Fig. 4E). The percentages of cells with diffuse PLZF/H3K9me3 staining were similar in the wild-type and *Dnmt3l* KO populations (Fig. 4D). Most of the H3K9me3 staining was colocalized with DAPI, suggesting that H3K9me3 were enriched in heterochromatin in both 8 dpp wild-type and *Dnmt3l* KO THY1⁺ cells (Fig. 4C). Of particular interest was a switch from a predominantly perinuclear staining pattern of PLZF and H3K9me3 in the wild-type THY1⁺ cells and the predominantly punctate staining pattern in the *Dnmt3l* KO THY1⁺ cells (Fig. 4D), indicating an enhanced tendency

towards proliferation in the THY1⁺ population in the absence of DNMT3L. Fewer than 10% of the wild-type and *Dnmt3l* KO PLZF⁺THY1⁺ cells exhibited both nuclear and cytoplasmic PLZF staining. The appearance of cytoplasmic PLZF was mostly associated with perinuclear PLZF staining. The intensity of the cytoplasmic PLZF in the wild-type cells was considerably stronger than in the *Dnmt3l* KO cells (see supplementary material Fig. S3). We subsequently isolated the nuclear/cytoplasmic fractions and quantified the PLZF in different subcellular locations. In 8 dpp wild-type THY1⁺ cells, 78±0.6% and 21.3±0.6% of the PLZF protein levels were in the nucleus and cytoplasm, respectively. PLZF was predominantly localized in the nuclei of *Dnmt3l* KO THY1⁺ cells.

An essential function for DNMT3L in PLZF stability

Although no clear difference in the levels of *Plzf* (*Zbtb16* – Mouse Genome Informatics) transcripts between prepubertal wild-type and *Dnmt3l* KO THY1⁺ cells was observed (Fig. 5A), the latter

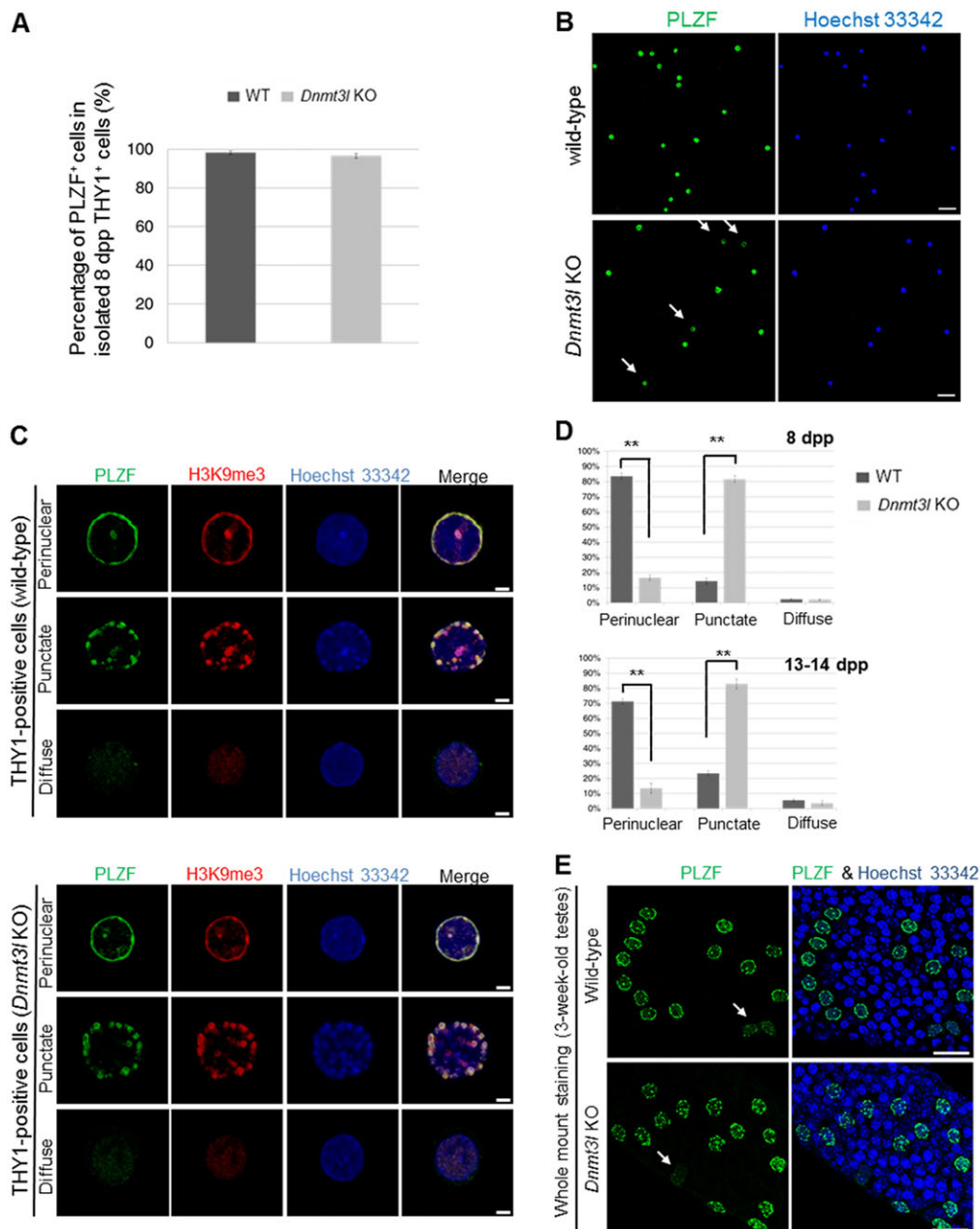


Fig. 4. Decrease in quiescent cells among the *Dnmt3l* KO THY1⁺ SPC population. (A) Percentages of PLZF⁺ cells in THY1⁺ cells isolated from 8 dpp wild-type and *Dnmt3l* KO testes. Data are mean±s.e.m. of six independent experiments. (B) Immunostaining of PLZF in 8 dpp THY1⁺ cells. Arrows indicate the THY1⁺ cells with weaker PLZF signals. Green, PLZF; blue, Hoechst 33342. Scale bars: 50 μm. (C) Immunostaining patterns of PLZF (green) and H3K9me3 (red) in 8 dpp wild-type and *Dnmt3l* KO THY1⁺ cells. Blue, Hoechst 33342. Scale bars: 2.5 μm. (D) Distribution of cells with perinuclear (quiescent), punctate (active) and diffuse H3K9me3 staining patterns in the various THY1⁺ PLZF⁺ cell populations. The results were compiled from approximately 600 randomly selected cells from six independent experiments. WT, wild type. (E) Whole-mount staining was performed on 3-week-old seminiferous tubules using an anti-PLZF antibody. The white arrows indicate A_{pr} spermatogonia with diffuse PLZF staining. Green, PLZF; blue, Hoechst 33342. Scale bars: 25 μm. Data are mean±s.e.m.; ***P*<0.01 (Student's *t*-test).

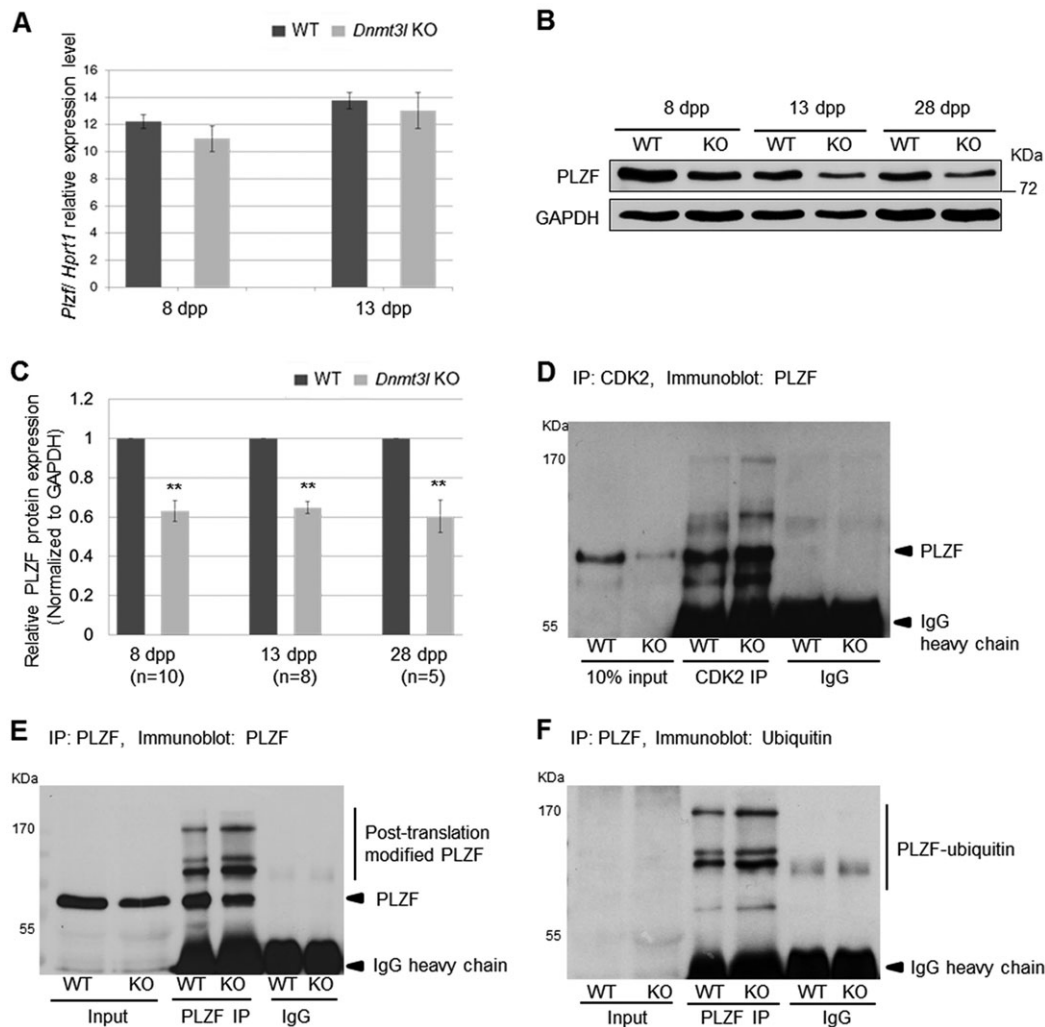


Fig. 5. Decreased PLZF expression and excessive PLZF ubiquitylation in *Dnmt3l* KO THY1⁺ cells. (A) Quantitative real-time PCR analysis of *Plzf* mRNA in postnatal wild-type and *Dnmt3l* KO THY1⁺ cells. The results (mean \pm s.e.m.) were calculated from three independent experiments. (B) Western blotting of PLZF in isolated THY1⁺ cells. Glyceraldehyde-3-phosphate-dehydrogenase (GAPDH) was used as an internal control. (C) Quantification of the PLZF protein expression levels in THY1⁺ cells. ** $P < 0.01$ (Student's *t*-test). Data are mean \pm s.e.m. of at least three independent experiments. *n*, the number of independently performed experiments. (D) Lysates from 8 dpp THY1⁺ cells were immunoprecipitated with an anti-CDK2 antibody and immunoblotted with an anti-PLZF antibody. (E,F) Lysates from 8 dpp THY1⁺ cells were immunoprecipitated with a monoclonal anti-PLZF antibody and immunoblotted with either the same anti-PLZF antibody (E) or an anti-ubiquitin antibody (F). Similar results were obtained from three independent experiments.

showed significantly reduced PLZF protein levels compared with wild-type cells (Fig. 5B,C), suggesting a potential post-translational regulatory role of DNMT3L in PLZF. *Dnmt3l* KO THY1⁺ cells exhibited increased CDK2 expression (Fig. 3C). CDK2 may phosphorylate PLZF, making it vulnerable to ubiquitylation-induced degradation (Costoya et al., 2008). After confirming the CDK2-PLZF interaction in THY1⁺ cells (Fig. 5D), we analyzed the post-translational modification of PLZF. PLZF was excessively post-translationally modified (Fig. 5E) and ubiquitylated (Fig. 5F) in 8 dpp *Dnmt3l* KO THY1⁺ cells, indicating that DNMT3L is involved in the regulation of PLZF stability in postnatal germ cells.

We further compared the PLZF expression levels of perinatal wild-type and *Dnmt3l* KO testes to clarify whether DNMT3L affects PLZF stability before the formation of the SPC pool. However, there was no clear difference of the low PLZF expression between wild-type and *Dnmt3l* KO testes at embryonic E18.5 or on the day of birth (see supplementary material Fig. S4). This was in contrast to the significant reduction in PLZF in postnatal

Dnmt3l KO THY1⁺ SPCs (Fig. 5B,C), suggesting that DNMT3L significantly affects PLZF stability only at postnatal stages.

Increased SALL4B levels and the SALL4A/PLZF ratio in *Dnmt3l* KO THY1⁺ cells

We next quantified two cell proliferation-promoting factors, SALL4A and SALL4B (Aguila et al., 2011; Oikawa et al., 2013), in wild-type and *Dnmt3l* KO germ cells. We observed strong SALL4B protein expression in wild-type testes from E17.5 to 8 dpp (Fig. 6A). However, in the prepubertal wild-type THY1⁺ SPC population, the SALL4B protein levels were dramatically downregulated (Fig. 6B,D and see supplementary material Fig. S5A,B), consistent with the reduced proliferative ability of this cell population. However, SALL4B expression was not suppressed in *Dnmt3l* KO THY1⁺ SPCs, suggesting that the suppression of SALL4B in SPCs may be DNMT3L dependent (Fig. 6B vs 6A).

The SALL4A/PLZF expression ratio is important for SPC cell fate determination (Hobbs et al., 2012). Compared with wild-type THY1⁺ cells, we observed a statistically significant upregulation of

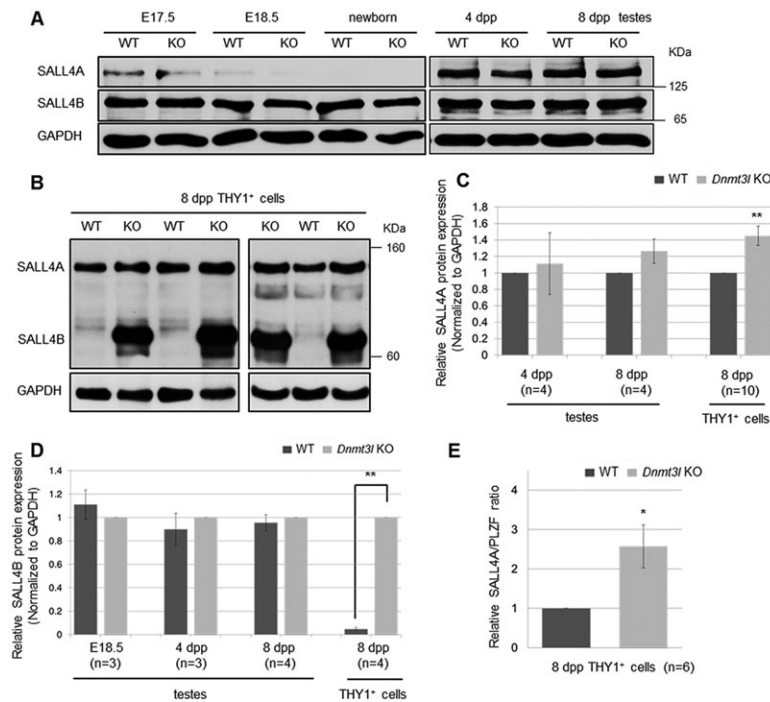


Fig. 6. Increased SALL4B expression and SALL4/PLZF ratio in *Dnmt3l* KO THY1⁺ cells. (A,B) Western blotting of SALL4A and SALL4B expression in E17.5 testes, E18.5 testes, newborn (0 dpp) testes, 4 dpp testes, 8 dpp testes and 8 dpp THY1⁺ cells using an anti-SALL4 antibody that detected both SALL4A and SALL4B. GAPDH was used as an internal control. (C) Quantification of the SALL4A protein expression levels in wild-type and *Dnmt3l* KO testes and THY1⁺ cells. (D) Relative SALL4B expression levels in E18.5 testes, 4 dpp testes, 8 dpp testes and 8 dpp THY1⁺ cells. The ratio of *Dnmt3l* KO SALL4B to GAPDH was normalized to one. (E) Bar chart displaying the ratio of SALL4A to PLZF in 8 dpp THY1⁺ cells. The results (mean±s.e.m.) were calculated from at least three independent experiments. * $P < 0.05$ and ** $P < 0.01$, respectively (Student's *t*-test). E, embryonic day; dpp, days postpartum.

the SALL4A protein in 8 dpp but not in 2-week-old *Dnmt3l* KO THY1⁺ SPCs (Fig. 6B,C and see supplementary material Fig. S5A). Along with the significant PLZF reduction in this mutant cell type (Fig. 5B,C), the SALL4/PLZF ratio was significantly increased in both 8 dpp and 2-week-old *Dnmt3l* KO THY1⁺ SPCs at the prepubertal stage (Fig. 6E and see supplementary material Fig. S5D), consistent with the increased non-quiescent THY1⁺ SPCs in prepubertal *Dnmt3l* KO testes.

We further investigated whether the increased SALL4 in *Dnmt3l* KO SPCs was associated with enhanced MEK-ERK and PTEN-AKT signaling cascades because the overexpression of SALL4 enhances the proliferation-stimulating AKT and ERK signal intensities (Yang et al., 2008b; Oikawa et al., 2009). PTEN protein levels were not significantly increased, but we observed a significant increase in PTEN phosphorylation (S380/T382/T383) (Fig. 7A,B), which restricts PTEN activity and results in increased AKT expression (Vazquez et al., 2000, 2001). We also observed increased AKT activation and excessive MEK-ERK activation in 8 dpp *Dnmt3l* KO THY1⁺ cells (Fig. 7A,B). The elevated phosphorylation of ERK and AKT proteins persisted in *Dnmt3l* KO THY1⁺ cells isolated from older mice (data not shown).

Thus, DNMT3L is required for the protection of PLZF from excessive ubiquitylation and for the appropriate SALL4-regulated signaling pathways.

Aberrant expression of proliferation- and differentiation-associated factors in *Dnmt3l* KO THY1⁺ cells

To further characterize the function of DNMT3L in SPC maintenance, we analyzed the expression of factors crucial for SPC cell cycling and differentiation. Compared with wild-type cells, 8 dpp *Dnmt3l* KO THY1⁺ cells displayed increased expression of ERK- and AKT-activated factors (*Gfra1*, *Ret*, *Nanos2* and *Etv5*) and of *Epcam*, an SPC differentiation-associated molecule. We also observed significantly decreased expression of *Ngn3*, *Pou3f1* and *Sohlh2*, which are essential for precise SPC differentiation (Fig. 7C). Thus, DNMT3L may be important for SPC cycling and may also be involved in their differentiation.

DISCUSSION

Many adult stem cells remain in a quiescent state as they wait to self-renew or to differentiate, suggesting a delicate balance between quiescence and cycling ensures tissue homeostasis (Kippin et al., 2005; Horsley et al., 2008; Gan et al., 2010; Matsumoto et al., 2011). A large proportion of SPCs are found in the quiescent phase of the cell cycle (Costoya et al., 2004; Sada et al., 2009). Recent findings indicate that quiescence is essential for preventing premature activation of SPCs and stem cell depletion (Bruscoli et al., 2012; Hobbs et al., 2012; Hu et al., 2013). We demonstrated that postnatal *Dnmt3l* KO GFP⁺ SPCs failed to repopulate busulfan-treated wild-type recipient testes (see supplementary material Fig. S6), suggesting that autonomous defects in these cells contribute to the germ cell exhaustion phenotype observed in *Dnmt3l* KO animals (Liao et al., 2012). The newly identified significant DNMT3L expression in THY1⁺ cells in this study suggested that DNMT3L may function directly at the postnatal stage. We further revealed that DNMT3L participates in the maintenance of THY1⁺ SPC quiescence at least partly through modulating *Cdk2* expression and PLZF stability, as well as through silencing proliferation-promoting SALL4B expression.

Stem cell maintenance is modulated by the appropriate extrinsic stimulation by the niche and intrinsic gene expression. We compared the transcriptome profiles of 8 dpp wild-type and *Dnmt3l* KO THY1⁺ SPCs and identified cell proliferation-related cascades, including the PI3K-AKT, RAS and MAPK signaling pathways that were among the most significantly differentially regulated pathways based on a KEGG analysis (see supplementary material Fig. S7A). We also selected 53 genes involved in SPC proliferation and differentiation to perform a classical gene set enrichment analysis (GSEA). The results revealed significant enrichment ($P < 0.0002$) of these genes, further indicating that DNMT3L plays a role in SPC maintenance (see supplementary material Fig. S7B). Our transcriptome profiles revealed that, apart from cell proliferation-related molecules, receptor-ligand interaction and cell adhesion molecules were clearly affected in *Dnmt3l* KO THY1⁺ SPCs compared with wild-type SPCs. The uneven distribution of SPCs in prepubertal *Dnmt3l* KO testes implies that

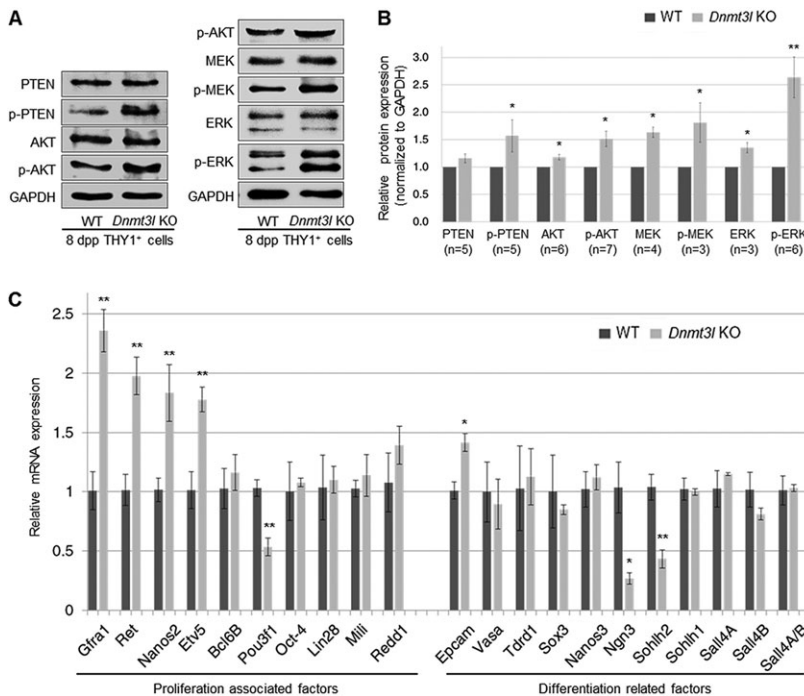


Fig. 7. Elevated ERK and AKT cascades in *Dnmt3l* KO THY1⁺ cells. (A) Increased activity of the AKT and ERK signaling pathways in 8 dpp *Dnmt3l* KO THY1⁺ cells. Western blotting of the expression and phosphorylation of molecules involved in the AKT and ERK signaling cascades. GAPDH was used as an internal control. (B) The relative expression of the AKT and ERK signaling molecules between 8 dpp wild-type and *Dnmt3l* KO THY1⁺ cells. Data are mean±s.e.m. from at least three independent experiments. *n*, the number of independent experiments. **P*<0.05 and ***P*<0.01, respectively (Student's *t*-test). (C) Quantitative real-time PCR analysis of genes associated with SPC proliferation and differentiation in 8 dpp wild-type and *Dnmt3l* KO THY1⁺ cells. Data are mean±s.e.m. from at least three independent experiments performed in triplicate. **P*<0.05, and ***P*<0.01 (Student's *t*-test).

DNMT3L may contribute to the maintenance of an adequate niche microenvironment. This dysregulated niche might be associated with a regulatory feedback loop through germ cell and niche cell communications (Zamudio et al., 2011), although further research into the contributions of DNMT3L to niche homeostasis at the prepubertal stage is needed.

CDK2 may be a key factor in the quiescence-proliferation decision (Spencer et al., 2013). A higher density of methylated DNA prevents ETS1-DNA binding and inhibits transcriptional activation (Maier et al., 2003; Chan et al., 2004). The upregulation of *Cdk2* in *Dnmt3l* KO THY1⁺ cells results from reduced DNMT3L-dependent CpG methylation at the distal CpG island of the *Cdk2* promoter. However, we cannot exclude the possibility that the hypomethylation of the *Cdk2* promoter in *Dnmt3l* KO THY1⁺ cells is partially a result of passive DNA demethylation due to excessive cell proliferation. In addition, the PHD-like domain in DNMT3L, which is responsible for recruiting histone modifiers, may also influence transcriptional control at the chromatin level (Aapola et al., 2002; Deplus et al., 2002).

PLZF can be regulated by CDK2-mediated PLZF degradation, by cytokine-influenced PLZF inactivation or by stress-induced PLZF degradation (Nanba et al., 2003; Costoya et al., 2008; Kang et al., 2008; Doulatov et al., 2009). Among these processes, only CDK2-mediated degradation does not lead to cytoplasmic PLZF accumulation. The lack of cytoplasmic PLZF accumulation in *Dnmt3l* KO THY1⁺ cells suggests that CDK2-mediated PLZF degradation occurs in these mutant cells.

Recent studies have demonstrated that extended AKT activity enhances SPC differentiation (Lee et al., 2007; Hasegawa et al., 2013) and that increases in both the ERK and AKT signaling cascades are associated with the premature exhaustion of SPCs (Bruscoli et al., 2012). In addition to increased proliferation, elevated AKT and ERK activities have been linked to deregulated spermatogenesis (Goertz et al., 2011; Ishii et al., 2012). PLZF may antagonize SALL4A activity in postnatal SPCs (Hobbs et al., 2012). SALL4 has been linked to the AKT and ERK signaling cascades, and has been implicated in the proliferation and differentiation of

several types of stem cells (Ma et al., 2006; Sakaki-Yumoto et al., 2006; Zhang et al., 2006; Yang et al., 2008a; Oikawa et al., 2009; Oikawa et al., 2013). For example, SALL4A or SALL4B overexpression in hematopoietic stem cells results in enhanced proliferation, but also in ineffective differentiation and excessive cell death (Ma et al., 2006; Aguila et al., 2011; Yang et al., 2011). Thus, the excessive PLZF ubiquitylation, dysregulated SALL4A and elevated SALL4B expression in *Dnmt3l* KO THY1⁺ cells suggest that DNMT3L affects PLZF stability and the ability of SALL4-mediated signaling cascades, including the AKT and ERK cascades, to regulate cell fate determination in mouse SPCs. In *Dnmt3l* KO SPCs, the aberrant expression of proliferation- and differentiation-related molecules leads to abnormally differentiated spermatogonia, followed by germ cell apoptosis at the spermatocyte stage (see supplementary material Fig. S8).

SALL4 interacts with DNMT3s, and SALL4 overexpression induces the DNA hypermethylation of its own promoter in the *in vitro* system (Yang et al., 2012b). However, there was no significant difference in *Sall4a* or *Sall4b* mRNA expression between 8 dpp wild-type and *Dnmt3l* KO THY1⁺ cells, which excludes the possibility of DNMT3L-mediated DNA methylation of the *Sall4* promoter and suggests that DNMT3L is crucial for the inhibition of SALL4 protein expression/accumulation in postnatal THY1⁺ cells. Moreover, SALL4A and SALL4B have distinct but overlapping functions; the two splice isoforms can bind to unique and overlapping promoter regions (Lu et al., 2009; Rao et al., 2010), which may account for the variable expression of SALL4 in *Dnmt3l* KO THY1⁺ cells. Recently, SALL4B stability was reported to be regulated through post-translational modifications (Yang et al., 2012a). Future investigations of DNMT3L-mediated cell type-specific SALL4 suppression should improve our understanding of mouse postnatal germline maintenance.

Redd1 (Ddit4 – Mouse Genome Informatics), a negative regulator of mammalian TOR complex 1 (mTORC1), is crucial for maintaining the undifferentiated state of SPCs (Hobbs et al., 2010). The downregulation of *Redd1* results in increased mTORC1 activity, the decreased expression of ERK-stimulated molecules (Gfra1 and

Ret) and decreased AKT activity in *Plzf* KO SPCs (Hobbs et al., 2010). In contrast, *Dnmt3l* KO SPCs exhibited no difference in *Redd1* expression but increased expression of *Gfra1*, *Ret* and AKT activity. This finding, which suggests that a lack of DNMT3L is dispensable for PLZF-mediated *Redd1* expression (which harnesses mTOR signaling), may account for the differences in proliferation tendency between *Dnmt3l* KO SPCs and *Plzf* KO SPCs.

Overexpression in SPCs of *Etv5*, a downstream molecule in the ERK pathway, causes defective differentiation of SPCs and blocks their development beyond the spermatocyte stage (Ishii et al., 2012). Moreover, SPCs maintain the capability to proliferate but do not properly differentiate when *Sohlh2* or *Ngn3* is silenced (Hao et al., 2008; Kaucher et al., 2012). We found that *Dnmt3l* KO THY1⁺ cells displayed significantly increased levels of *Etv5* and decreased levels of *Sohlh2* transcripts. Furthermore, similar to findings in *Sohlh2* KO testes (Hao et al., 2008; Suzuki et al., 2012), *Dnmt3l* KO THY1⁺ cells exhibited upregulated expression of ERK-stimulated genes (*Gfra1*, *Ret* and *Nanos2*) (Hasegawa et al., 2013) and downregulated *Ngn3* expression. Thus, DNMT3L may be important for SPC cycling and could play a role in SPC differentiation.

In addition to inhibiting excessive SPC activation, DNMT3L and PLZF are both essential for transposable element (TE) silencing to repress TE mobility/propagation and to maintain genomic integrity in germ cells (Bourc'his and Bestor, 2004; Hata et al., 2006; Puszyk et al., 2013). PLZF is crucial for recruiting histone deacetylase (HDAC) and DNMT in order to inactivate retrotransposon expression (Puszyk et al., 2013). Importantly, DNMT3L co-precipitated with PLZF in THY1⁺ cells (H.-F.L. and S.-P.L., unpublished observation). Future investigations of DNMT3L/PLZF-mediated mechanisms should elucidate epigenetic TE silencing in SPCs.

Based on our preliminary genome-wide DNA methylation analysis, there was no major difference in overall DNA methylation levels between wild-type and *Dnmt3l* KO THY1⁺ cells at 8 dpp. As described by Kato et al. (2007) and Niles et al. (2011), DNMT3L deficiency fails to install DNA methylation properly in prenatal male germ cells. Therefore, perinatal *Dnmt3l* KO male germ cells are globally hypomethylated compared with their wild-type counterparts (Kato et al., 2007; Oakes et al., 2007). However, DNA methylation continues to be installed in postnatal *Dnmt3l* KO germ cells. By 6 dpp, *Dnmt3l* KO spermatogonia have similar global DNA methylation levels compared to their wild-type counterparts (Niles et al., 2011).

Despite their similar global DNA methylation state, 8 dpp *Dnmt3l* KO THY1⁺ cells were hypomethylated at paternally methylated imprinting control regions (including IG-DMR, *Rasgrf1*-DMR and *H19*-DMR) and TEs compared with 8 dpp wild-type THY1⁺ cells (data not shown). The hypomethylation of TEs in *Dnmt3l* KO THY1⁺ cells was associated with an upregulation of *LINE1*-ORF1 and *IAPGAG* expressions compared with the wild-type littermate control (see supplementary material Fig. S9). These data suggest that DNMT3L is particularly important for the dosage regulation of imprinted genes and TEs in both embryonic and postnatal germ cells.

DNMT3L may play different roles in male germ cell development at different stages. In prenatal prospermatogonia, the timing of DNMT3L expression starts after the cells enter mitotic arrest (E14.5 to newborn). There is no obvious difference in germ cell number between wild-type and *Dnmt3l* KO testes at the perinatal stage (Bourc'his et al., 2001; Sakai et al., 2004). This is in contrast to the over-proliferating THY1⁺ SPC population in the absence of DNMT3L from 8 dpp onwards after SPCs re-enter cell cycling, partly due to DNMT3L-modulated CDK2 dosage and PLZF stability. These findings suggest that DNMT3L may

be dispensable for quiescence establishment/maintenance at the embryonic stage. Our results revealed that, compared with 8 dpp wild-type THY1⁺ cells, the expression levels of *Cdk2* were equally very low in both embryonic wild-type and *Dnmt3l* KO prospermatogonia (data not shown), indicating that DNMT3L does not participate in cyclin/CDK-mediated cell cycle modulation in quiescent embryonic prospermatogonia. In contrast, beginning at 8 dpp, our results revealed clearly dysregulated SPC proliferation in *Dnmt3l* KO testes, indicating that postnatal DNMT3L contributes to the cell fate determination of SPCs when they have matured from prospermatogonia. DNMT3L may also be involved in different complexes and participate in different mechanisms for proper germ cell development at different stages. Our results show that PLZF interacts with DNMT3L and CDK2 in 8 dpp wild-type THY1⁺ cells; however, PLZF and CDK2 were weakly expressed in the perinatal germ cells. The lack of a significant difference in the expressions of these molecules between perinatal wild-type and *Dnmt3l* KO germ cells implies that DNMT3L may not be responsible for their expression or function throughout embryonic germ cell development.

In addition to germ cells and preimplantation embryos, DNMT3L has recently been shown to be expressed in hematopoietic stem/progenitor cells (HSCs) and may be involved in SALL4-mediated transcriptional regulation of HSC differentiation (Liu et al., 2013). However, the potential function of DNMT3L in regulating HSC quiescence and maintenance remains unclear. Recent studies have revealed that PLZF and SALL4 are expressed in HSCs, in which PLZF contributes to tumor suppression (He et al., 2000; Ono et al., 2013), and that SALL4 overexpression leads to HSC over-proliferation (Yang et al., 2011). In this study, a lack of DNMT3L in the relatively quiescent THY1⁺ SPCs resulted in increased proliferation, which was associated with PLZF instability and upregulated SALL4-mediated proliferation cascades. The functions of DNMT3L in SPC quiescence and potentially niche homeostasis may be applicable to other somatic stem cells.

In conclusion, our results suggest that DNMT3L has a crucial function in modulating the cell fate of quiescent THY1⁺ SPCs in postnatal testes. Our findings support a novel role for DNMT3L in SPCs to ensure the lifelong maintenance of the germline pool.

MATERIALS AND METHODS

Germ cell isolation and flow cytometry

Mice heterozygous for the *Dnmt3l*^{m1Enls} mutant allele (Hata et al., 2002) were intercrossed to generate *Dnmt3l* KO pups and littermate controls. Five postnatal mice of the same genotype were used for each experiment. Seminiferous tubules were treated with collagenase IV and DNase I to remove interstitial Leydig cells and peritubular myoid cells, followed by trypsin digestion to generate cell suspensions (Ogawa et al., 1997). THY1⁺ cells were isolated by magnetic-activated cell sorting (MACS) (Miltenyi Biotec), following the manufacturer's instructions. Briefly, the dispersed testicular cells were placed in the MACS buffer and incubated with a biotin-conjugated anti-CD90.2 (THY1) antibody (Lot 25136 and Lot 80806, 553011, BD Pharmingen) at 4°C for 10 min. After being washed, the cells were resuspended, labeled with anti-biotin microbeads (Miltenyi Biotec) at 4°C for 15 min and placed in collection tubes for isolation. The isolation process was carried out within 5 h to maximize the amount of living cells. A PE-Cy5-conjugated anti-CD49f antibody (551129, BD Pharmingen) was used for the SPC population analysis. The date of birth for timed postnatal mice was defined as 0 dpp.

Quantitative reverse transcription PCR

Reverse transcription reactions and qPCR were performed using a SuperScript First-Strand Synthesis System (Invitrogen) and Roche Light-Cycler 480II. Primers are listed in Table S1 of the supplementary material.

Immunohistochemistry and immunocytochemistry

Mouse testes were fixed with 4% paraformaldehyde (PFA), transferred into sucrose gradients for dehydration, embedded in OCT compound (Tissue-Tek O.C.T. Compound) and cut into 8 μ m sections. The sections were blocked with 10% goat serum before incubation with primary antibodies (a dilution of 1:1000), anti-PLZF (sc-22839, Santa Cruz Biotechnology) and anti-H3K9me3 (ab8898, Abcam). For whole-mount staining, seminiferous tubules were digested with collagenase IV and fixed in 4% PFA. For immunocytochemistry, the isolated THY1⁺ cells were placed onto poly-L-lysine slides (Thermo Scientific) and fixed in 4% PFA. Samples (testis sections, seminiferous tubules and isolated THY1⁺ cells) were washed with PBS, treated with 0.5% Triton X-100 in PBS and blocked in 10% goat serum with 1-2% bovine serum albumin (BSA). After incubation with the primary antibodies, sections and tubules were incubated with secondary antibodies (a dilution of 1:500, 715-485-150, DyLight 488 and 211-505-109 DyLight 549, Jackson ImmunoResearch), stained with Hoechst 33342 (Sigma) and mounted with a mounting medium (P36934, Invitrogen). The specificity of the PLZF antibody was evaluated using testes from wild-type and homozygous luxoid (*Plzf*^{lu/lu}) mice at 8 dpp (Buaas et al., 2004) (see supplementary material Fig. S10).

Chromatin immunoprecipitation (ChIP)

ChIP assays were performed using a LowCell# ChIP kit (Diagenode). Briefly, 1 \times 10⁶ freshly isolated THY1⁺ cells were cross-linked using 1% formaldehyde for 10 min at room temperature; the cross-linking was arrested with glycine. After centrifugation, the cells were resuspended in a lysis buffer and the genomic DNA was sheared to lengths of approximately 500 bp by ultrasound. The sheared chromatin was incubated with 4 μ g of anti-ETS1 (sc-350, Santa Cruz Biotechnology), anti-H3K4me3 (ab8580, Abcam), anti-H3K27me3 (07-449, Millipore) or control IgGs (Diagenode) overnight at 4°C with rotation. The immunoprecipitated DNA was isolated using DNA isolation buffer (Diagenode). Specific genes in the purified DNA were qPCR-amplified and analyzed.

Immunoprecipitation and western blotting

Isolated THY1⁺ cells and testes were lysed in RIPA buffer (Millipore) supplemented with 1 \times protease inhibitor cocktail (R1321, Fermentas), 1 \times phosphatase inhibitor cocktail (524629, Millipore), and 1 mM PMSF. Immunoprecipitation was performed using a Dynabeads kit (Invitrogen) following the manufacturer's protocol. The anti-PLZF- and anti-CDK2-coated Dynabead/protein mixture was gently rotated overnight at 4°C. For immunoprecipitation, 50 μ g of total protein from wild-type and Dnmt3l KO THY1⁺ cells were used for each experiment. Western blotting was performed according to a standard protocol (Sambrook and Russell, 2001) using PVDF membranes (Millipore). Cell or tissue extracts (10-15 μ g per lane) were prepared for analysis. The membranes were blocked with a blocker (Bl κ -PO or Bl κ -CH, Millipore) or 5% BSA (Sigma), except for the membrane incubated with the anti-DNMT3L antibody, which was blocked with Bl κ -PO and then switched to 5% milk in 1 \times PBST. Please note that an extended protocol is necessary for detecting DNMT3L from THY1⁺ SPCs as there are strong non-specific signals with a molecular weight similar to DNMT3L in this cell type. A detailed anti-DNMT3L signal detection protocol is provided in the supplementary materials and methods. A regular western blot protocol is applicable to embryonic stem cells or embryonic testes. The incubations with the primary antibodies (a dilution of 1:1000) were performed at 4°C overnight with gentle shaking. The membranes were incubated with a horseradish peroxidase-conjugated secondary antibody (Pierce). The proteins were detected using a chemiluminescent reagent (Millipore), and the images were quantified using ImageJ software (<http://rsbweb.nih.gov/ij/>) and a BioSpectrum Imaging System (UVP). The antibodies used are listed in supplementary material Table S2.

DNA extraction and bisulfite sequencing

Genomic DNA was extracted from THY1⁺ cells and treated using an EZ DNA methylation kit (Zymo Research). The PCR products were purified and cloned for subsequent sequencing.

CD49f+GSC culture, transfection and luciferase assay

DNA segments of the *Cdk2* promoter were amplified, purified and cloned to generate promoter reporter plasmids. Mouse AP⁺ GSCs were derived from newborn testes as previously described (Huang et al., 2009). Cells were electroporated, seeded onto a laminin-coated plate and cultured using a serum-free basic system for 48 h. The luciferase activity was determined and recorded with a Berthold LB 960 Centro microplate luminometer (Berthold Technologies).

RNA Sequencing and bioinformatics analysis

Total RNA for the library preparation, sequencing and RNA-Seq analysis was extracted using TRI Reagent (Ambion). Poly-T oligo-attached magnetic beads were used to purify RNA. The mRNA was fragmented into small pieces and copied into first-strand cDNA, followed by second-strand cDNA synthesis. These cDNA fragments underwent end-repair, a single A base addition and adapter ligation to create the final cDNA library. Paired-end 100-nucleotide reads were obtained using HiScanSQ (Illumina). The sequences have been deposited in the NCBI GEO database under the accession number GSE54411.

Detailed experimental protocols are provided in the supplementary materials and methods.

Acknowledgements

The authors are sincerely grateful to Prof Anne Ferguson-Smith (Cambridge University, UK) for useful discussions; and to Dr Xing Zhang and Dr Xiaodong Cheng (Emory University, USA) for kindly providing the anti-DNMT3L antibodies.

Competing interests

The authors declare no competing financial interests.

Author contributions

H.-F.L., W.S.C.C., P.Y., Y.-H.H. and S.-P.L. conceived and designed the experiments; K.H., H.S. and Y.-H. Ching provided study materials; H.-F.L., Y.-H. Chen, W.S.C.C., P.-L.L., C.-Y.L., Y.-C.C., Q.-J.L., Y.-T.T., M.-H.T. and T.-H.K. performed the experiments and assembled and analyzed the data; H.-F.L., W.S.C.C., W.T.K.C., P.Y., Y.-H.H., S.-C.W. and S.-P.L. interpreted the data; and H.-F.L., W.S.C.C., P.Y. and S.-P.L. wrote the manuscript with support from H.-N.H., Y.-H. Ching and Y.-H.H. All authors were involved in discussions and approved the final manuscript.

Funding

This work was supported by grants from the Ministry of Science and Technology [99-3111-B-002-008, 101-2321-B-002-037 and 102-2321-B-002-031 to S.-P.L.] and National Taiwan University [NTU-CESRP-102R7602D3 to S.-P.L.] and by intramural support from the Academia Sinica to P.Y. Deposited in PMC for immediate release.

Supplementary material

Supplementary material available online at <http://dev.biologists.org/lookup/suppl/doi:10.1242/dev.105130/-DC1>

References

- Aapola, U., Shibuya, K., Scott, H. S., Ollila, J., Vihinen, M., Heino, M., Shintani, A., Kawasaki, K., Minoshima, S., Krohn, K. et al. (2000). Isolation and initial characterization of a novel zinc finger gene, DNMT3L, on 21q22.3, related to the cytosine-5-methyltransferase 3 gene family. *Genomics* **65**, 293-298.
- Aapola, U., Lyle, R., Krohn, K., Antonarakis, S. E. and Peterson, P. (2001). Isolation and initial characterization of the mouse Dnmt3l gene. *Cytogenet. Cell Genet.* **92**, 122-126.
- Aapola, U., Liiv, I. and Peterson, P. (2002). Imprinting regulator DNMT3L is a transcriptional repressor associated with histone deacetylase activity. *Nucleic Acids Res.* **30**, 3602-3608.
- Aguila, J. R., Liao, W., Yang, J., Avila, C., Hagag, N., Senzel, L. and Ma, Y. (2011). SALL4 is a robust stimulator for the expansion of hematopoietic stem cells. *Blood* **118**, 576-585.
- Arand, J., Spieler, D., Karius, T., Branco, M. R., Meilinger, D., Meissner, A., Jenuwein, T., Xu, G., Leonhardt, H., Wolf, V. et al. (2012). In vivo control of CpG and non-CpG DNA methylation by DNA methyltransferases. *PLoS Genet.* **8**, e1002750.
- Bourc'his, D. and Bestor, T. H. (2004). Meiotic catastrophe and retrotransposon reactivation in male germ cells lacking Dnmt3L. *Nature* **431**, 96-99.
- Bourc'his, D., Xu, G.-L., Lin, C.-S., Bollman, B. and Bestor, T. H. (2001). Dnmt3L and the establishment of maternal genomic imprints. *Science* **294**, 2536-2539.

- Bruscoli, S., Velardi, E., Di Sante, M., Bereshchenko, O., Venanzi, A., Coppo, M., Berno, V., Mamelì, M. G., Colella, R., Cavaliere, A. et al. (2012). Long glucocorticoid-induced leucine zipper (L-GILZ) protein interacts with ras protein pathway and contributes to spermatogenesis control. *J. Biol. Chem.* **287**, 1242-1251.
- Buaas, F. W., Kirsh, A. L., Sharma, M., McLean, D. J., Morris, J. L., Griswold, M. D., de Rooij, D. G. and Braun, R. E. (2004). Plzf is required in adult male germ cells for stem cell self-renewal. *Nat. Genet.* **36**, 647-652.
- Chan, Y., Fish, J. E., D'Abreo, C., Lin, S., Robb, G. B., Teichert, A.-M., Karantzoulis-Fegaras, F., Keightley, A., Steer, B. M. and Marsden, P. A. (2004). The cell-specific expression of endothelial nitric-oxide synthase: a role for DNA methylation. *J. Biol. Chem.* **279**, 35087-35100.
- Chedin, F., Lieber, M. R. and Hsieh, C.-L. (2002). The DNA methyltransferase-like protein DNMT3L stimulates de novo methylation by Dnmt3a. *Proc. Natl. Acad. Sci. U.S.A.* **99**, 16916-16921.
- Cheung, T. H. and Rando, T. A. (2013). Molecular regulation of stem cell quiescence. *Nat. Rev. Mol. Cell Biol.* **14**, 329-340.
- Costoya, J. A., Hobbs, R. M., Barna, M., Cattoretti, G., Manova, K., Sukhwani, M., Orwig, K. E., Wolgemuth, D. J. and Pandolfi, P. P. (2004). Essential role of Plzf in maintenance of spermatogonial stem cells. *Nat. Genet.* **36**, 653-659.
- Costoya, J. A., Hobbs, R. M. and Pandolfi, P. P. (2008). Cyclin-dependent kinase antagonizes promyelocytic leukemia zinc-finger through phosphorylation. *Oncogene* **27**, 3789-3796.
- Deplus, R., Brenner, C., Burgers, W. A., Putmans, P., Kouzarides, T., de Launoit, Y. and Fuks, F. (2002). Dnmt3L is a transcriptional repressor that recruits histone deacetylase. *Nucleic Acids Res.* **30**, 3831-3838.
- Doulatov, S., Notta, F., Rice, K. L., Howell, L., Zelent, A., Licht, J. D. and Dick, J. E. (2009). PLZF is a regulator of homeostatic and cytokine-induced myeloid development. *Genes Dev.* **23**, 2076-2087.
- Ema, H. and Suda, T. (2012). Two anatomically distinct niches regulate stem cell activity. *Blood* **120**, 2174-2181.
- Gan, B., Hu, J., Jiang, S., Liu, Y., Sahin, E., Zhuang, L., Fletcher-Sanankone, E., Colla, S., Wang, Y. A., Chin, L. et al. (2010). Lkb1 regulates quiescence and metabolic homeostasis of haematopoietic stem cells. *Nature* **468**, 701-704.
- Gasse, K. and Orwig, K. E. (2013). SALL4 expression in gonocytes and spermatogonial clones of postnatal mouse testes. *PLoS ONE* **8**, e53976.
- Goertz, M. J., Wu, Z., Gallardo, T. D., Hamra, F. K. and Castrillon, D. H. (2011). Foxo1 is required in mouse spermatogonial stem cells for their maintenance and the initiation of spermatogenesis. *J. Clin. Invest.* **121**, 3456-3466.
- Hao, J., Yamamoto, M., Richardson, T. E., Chapman, K. M., Denard, B. S., Hammer, R. E., Zhao, G. Q. and Hamra, F. K. (2008). Sohlh2 knockout mice are male-sterile because of degeneration of differentiating type A spermatogonia. *Stem Cells* **26**, 1587-1597.
- Hasegawa, K., Namekawa, S. H. and Saga, Y. (2013). MEK/ERK signaling directly and indirectly contributes to the cyclical self-renewal of spermatogonial stem cells. *Stem Cells* **31**, 2517-2527.
- Hata, K., Okano, M., Lei, H. and Li, E. (2002). Dnmt3L cooperates with the Dnmt3 family of de novo DNA methyltransferases to establish maternal imprints in mice. *Development* **129**, 1983-1993.
- Hata, K., Kusumi, M., Yokomine, T., Li, E. and Sasaki, H. (2006). Meiotic and epigenetic aberrations in Dnmt3L-deficient male germ cells. *Mol. Reprod. Dev.* **73**, 116-122.
- He, L.-Z., Bhaumik, M., Tribioli, C., Rego, E. M., Ivins, S., Zelent, A. and Pandolfi, P. P. (2000). Two critical hits for promyelocytic leukemia. *Mol. Cell* **6**, 1131-1141.
- Heinemeyer, T., Wingender, E., Reuter, I., Hermjakob, H., Kel, A. E., Kel, O. V., Ignatieva, E. V., Ananko, E. A., Podkolodnaya, O. A., Kolpakov, F. A. et al. (1998). Databases on transcriptional regulation: TRANSFAC, TRRD and COMPEL. *Nucleic Acids Res.* **26**, 362-367.
- Hobbs, R. M., Seandel, M., Falcatori, I., Rafii, S. and Pandolfi, P. P. (2010). Plzf regulates germline progenitor self-renewal by opposing mTORC1. *Cell* **142**, 468-479.
- Hobbs, R. M., Fagoonee, S., Papa, A., Webster, K., Altruda, F., Nishinakamura, R., Chai, L. and Pandolfi, P. P. (2012). Functional antagonism between Sall4 and Plzf defines germline progenitors. *Cell Stem Cell* **10**, 284-298.
- Holz-Schietinger, C. and Reich, N. O. (2010). The inherent processivity of the human de novo methyltransferase 3A (DNMT3A) is enhanced by DNMT3L. *J. Biol. Chem.* **285**, 29091-29100.
- Horsley, V., Aliprantis, A. O., Polak, L., Glimcher, L. H. and Fuchs, E. (2008). NFATc1 balances quiescence and proliferation of skin stem cells. *Cell* **132**, 299-310.
- Hu, Y.-C., de Rooij, D. G. and Page, D. C. (2013). Tumor suppressor gene Rb is required for self-renewal of spermatogonial stem cells in mice. *Proc. Natl. Acad. Sci. U.S.A.* **110**, 12685-12690.
- Huang, Y.-H., Chin, C.-C., Ho, H.-N., Chou, C.-K., Shen, C.-N., Kuo, H.-C., Wu, T.-J., Wu, Y.-C., Hung, Y.-C., Chang, C.-C. et al. (2009). Pluripotency of mouse spermatogonial stem cells maintained by IGF-1-dependent pathway. *FASEB J.* **23**, 2076-2087.
- Ichiyanagi, T., Ichiyanagi, K., Miyake, M. and Sasaki, H. (2013). Accumulation and loss of asymmetric non-CpG methylation during male germ-cell development. *Nucleic Acids Res.* **41**, 738-745.
- Ishii, K., Kanatsu-Shinohara, M., Toyokuni, S. and Shinohara, T. (2012). FGF2 mediates mouse spermatogonial stem cell self-renewal via upregulation of Etv5 and Bcl6b through MAP2K1 activation. *Development* **139**, 1734-1743.
- Jia, D., Jurkowska, R. Z., Zhang, X., Jeltsch, A. and Cheng, X. (2007). Structure of Dnmt3a bound to Dnmt3L suggests a model for de novo DNA methylation. *Nature* **449**, 248-251.
- Kang, S. I., Choi, H. W. and Kim, I. Y. (2008). Redox-mediated modification of PLZF by SUMO-1 and ubiquitin. *Biochem. Biophys. Res. Commun.* **369**, 1209-1214.
- Kato, Y., Kaneda, M., Hata, K., Kumaki, K., Hisano, M., Kohara, Y., Okano, M., Li, E., Nozaki, M. and Sasaki, H. (2007). Role of the Dnmt3 family in de novo methylation of imprinted and repetitive sequences during male germ cell development in the mouse. *Hum. Mol. Genet.* **16**, 2272-2280.
- Kaucher, A. V., Oatley, M. J. and Oatley, J. M. (2012). NEUROG3 is a critical downstream effector for STAT3-regulated differentiation of mammalian stem and progenitor spermatogonia. *Biol. Reprod.* **86**, 164.
- Kippin, T. E., Martens, D. J. and van der Kooy, D. (2005). p21 loss compromises the relative quiescence of forebrain stem cell proliferation leading to exhaustion of their proliferation capacity. *Genes Dev.* **19**, 756-767.
- Kobayashi, H., Sakurai, T., Imai, M., Takahashi, N., Fukuda, A., Yayoi, O., Sato, S., Nakabayashi, K., Hata, K., Sotomaru, Y. et al. (2012). Contribution of intragenic DNA methylation in mouse gametic DNA methylomes to establish oocyte-specific heritable marks. *PLoS Genet.* **8**, e1002440.
- La Salle, S., Mertineit, C., Taketo, T., Moens, P. B., Bestor, T. H. and Trasler, J. M. (2004). Windows for sex-specific methylation marked by DNA methyltransferase expression profiles in mouse germ cells. *Dev. Biol.* **268**, 403-415.
- La Salle, S., Oakes, C. C., Neaga, O. R., Bourc'his, D., Bestor, T. H. and Trasler, J. M. (2007). Loss of spermatogonia and wide-spread DNA methylation defects in newborn male mice deficient in DNMT3L. *BMC Dev. Biol.* **7**, 104.
- Lee, J., Kanatsu-Shinohara, M., Inoue, K., Ogonuki, N., Miki, H., Toyokuni, S., Kimura, T., Nakano, T., Ogura, A. and Shinohara, T. (2007). Akt mediates self-renewal division of mouse spermatogonial stem cells. *Development* **134**, 1853-1859.
- Liao, H.-F., Tai, K.-Y., Chen, W. S.-C., Cheng, L. C.-W., Ho, H.-N. and Lin, S.-P. (2012). Functions of DNA methyltransferase 3-like in germ cells and beyond. *Biol. Cell* **104**, 571-587.
- Liu, L., Souto, J., Liao, W., Jiang, Y., Li, Y., Nishinakamura, R., Huang, S., Rosengart, T., Yang, V. W., Schuster, M. et al. (2013). Histone lysine-specific demethylase 1 (LSD1) protein is involved in Sall-like protein 4 (SALL4)-mediated transcriptional repression in hematopoietic stem cells. *J. Biol. Chem.* **288**, 34719-34728.
- Lu, J., Jeong, H. W., Kong, N., Yang, Y., Carroll, J., Luo, H. R., Silberstein, L. E., Ma, Y. and Chai, L. (2009). Stem cell factor SALL4 represses the transcriptions of PTEN and SALL1 through an epigenetic repressor complex. *PLoS ONE* **4**, e5577.
- Ma, Y., Cui, W., Yang, J., Qu, J., Di, C., Amin, H. M., Lai, R., Ritz, J., Krause, D. S. and Chai, L. (2006). SALL4, a novel oncogene, is constitutively expressed in human acute myeloid leukemia (AML) and induces AML in transgenic mice. *Blood* **108**, 2726-2735.
- Mahadevaiah, S. K., Bourc'his, D., de Rooij, D. G., Bestor, T. H., Turner, J. M. A. and Burgoyne, P. S. (2008). Extensive meiotic asynapsis in mice antagonizes meiotic silencing of unsynapsed chromatin and consequently disrupts meiotic sex chromosome inactivation. *J. Cell Biol.* **182**, 263-276.
- Maier, H., Colbert, J., Fitzsimmons, D., Clark, D. R. and Hagman, J. (2003). Activation of the early B-cell-specific mb-1 (Ig-alpha) gene by Pax-5 is dependent on an unmethylated Ets binding site. *Mol. Cell. Biol.* **23**, 1946-1960.
- Matsumoto, A., Takeishi, S., Kanie, T., Susaki, E., Onoyama, I., Tateishi, Y., Nakayama, K. and Nakayama, K. I. (2011). p57 is required for quiescence and maintenance of adult hematopoietic stem cells. *Cell Stem Cell* **9**, 262-271.
- McConnell, M. J., Chevallier, N., Berkofsky-Fessler, W., Giltane, J. M., Malani, R. B., Staudt, L. M. and Licht, J. D. (2003). Growth suppression by acute promyelocytic leukemia-associated protein PLZF is mediated by repression of c-myc expression. *Mol. Cell. Biol.* **23**, 9375-9388.
- Nakagawa, T., Nabeshima, Y.-i. and Yoshida, S. (2007). Functional identification of the actual and potential stem cell compartments in mouse spermatogenesis. *Dev. Cell* **12**, 195-206.
- Nakagawa, T., Sharma, M., Nabeshima, Y.-i., Braun, R. E. and Yoshida, S. (2010). Functional hierarchy and reversibility within the murine spermatogenic stem cell compartment. *Science* **328**, 62-67.
- Nanba, D., Mammoto, A., Hashimoto, K. and Higashiyama, S. (2003). Proteolytic release of the carboxy-terminal fragment of proHB-EGF causes nuclear export of PLZF. *J. Cell Biol.* **163**, 489-502.
- Niles, K. M., Chan, D., La Salle, S., Oakes, C. C. and Trasler, J. M. (2011). Critical period of nonpromoter DNA methylation acquisition during prenatal male germ cell development. *PLoS ONE* **6**, e24156.
- Oakes, C. C., La Salle, S., Smiraglia, D. J., Robaire, B. and Trasler, J. M. (2007). A unique configuration of genome-wide DNA methylation patterns in the testis. *Proc. Natl. Acad. Sci. U.S.A.* **104**, 228-233.

- Oatley, J. M. and Brinster, R. L. (2012). The germline stem cell niche unit in mammalian testes. *Physiol. Rev.* **92**, 577-595.
- Ogawa, T., Arechaga, J. M., Avarbock, M. R. and Brinster, R. L. (1997). Transplantation of testis germinal cells into mouse seminiferous tubules. *Int. J. Dev. Biol.* **41**, 111-122.
- Oikawa, T., Kamiya, A., Kakinuma, S., Zeniya, M., Nishinakamura, R., Tajiri, H. and Nakauchi, H. (2009). Sall4 regulates cell fate decision in fetal hepatic stem/progenitor cells. *Gastroenterology* **136**, 1000-1011.
- Oikawa, T., Kamiya, A., Zeniya, M., Chikada, H., Hyuck, A. D., Yamazaki, Y., Wauthier, E., Tajiri, H., Miller, L. D., Wang, X. W. et al. (2013). Sal-like protein 4 (SALL4), a stem cell biomarker in liver cancers. *Hepatology* **57**, 1469-1483.
- Ono, R., Masuya, M., Nakajima, H., Enomoto, Y., Miyata, E., Nakamura, A., Ishii, S., Suzuki, K., Shibata-Minoshima, F., Katayama, N. et al. (2013). Plzf drives MLL-fusion-mediated leukemogenesis specifically in long-term hematopoietic stem cells. *Blood* **122**, 1271-1283.
- Ooi, S. K., Qiu, C., Bernstein, E., Li, K., Jia, D., Yang, Z., Erdjument-Bromage, H., Tempst, P., Lin, S.-P., Allis, C. D. et al. (2007). DNMT3L connects unmethylated lysine 4 of histone H3 to de novo methylation of DNA. *Nature* **448**, 714-717.
- Orford, K. W. and Scadden, D. T. (2008). Deconstructing stem cell self-renewal: genetic insights into cell-cycle regulation. *Nat. Rev. Genet.* **9**, 115-128.
- Payne, C. and Braun, R. E. (2006). Histone lysine trimethylation exhibits a distinct perinuclear distribution in Plzf-expressing spermatogonia. *Dev. Biol.* **293**, 461-472.
- Puszyk, W., Down, T., Grimwade, D., Chomienne, C., Oakey, R. J., Solomon, E. and Guidez, F. (2013). The epigenetic regulator PLZF represses L1 retrotransposition in germ and progenitor cells. *EMBO J.* **32**, 1941-1952.
- Rao, S., Zhen, S., Roumiantsev, S., McDonald, L. T., Yuan, G.-C. and Orkin, S. H. (2010). Differential roles of Sall4 isoforms in embryonic stem cell pluripotency. *Mol. Cell. Biol.* **30**, 5364-5380.
- Rice, K. L., Hormaeche, I., Doulatov, S., Flatow, J. M., Grimwade, D., Mills, K. I., Leiva, M., Ablain, J., Ambardekar, C., McConnell, M. J. et al. (2009). Comprehensive genomic screens identify a role for PLZF-RARalpha as a positive regulator of cell proliferation via direct regulation of c-MYC. *Blood* **114**, 5499-5511.
- Sada, A., Suzuki, A., Suzuki, H. and Saga, Y. (2009). The RNA-binding protein NANOS2 is required to maintain murine spermatogonial stem cells. *Science* **325**, 1394-1398.
- Sakai, Y., Suetake, I., Shinozaki, F., Yamashina, S. and Tajima, S. (2004). Co-expression of de novo DNA methyltransferases Dnmt3a2 and Dnmt3L in gonocytes of mouse embryos. *Gene Expr. Patterns* **5**, 231-237.
- Sakaki-Yumoto, M., Kobayashi, C., Sato, A., Fujimura, S., Matsumoto, Y., Takasato, M., Kodama, T., Aburatani, H., Asashima, M., Yoshida, N. et al. (2006). The murine homolog of SALL4, a causative gene in Okhiro syndrome, is essential for embryonic stem cell proliferation, and cooperates with Sall1 in anorectal, heart, brain and kidney development. *Development* **133**, 3005-3013.
- Sambrook, J. and Russell, D. W. (2001). *Molecular Cloning: A Laboratory Manual*, 3rd edn. New York, USA: Cold Spring Harbor Laboratory Press.
- Smallwood, S. A., Tomizawa, S.-I., Krueger, F., Ruf, N., Carli, N., Segonds-Pichon, A., Sato, S., Hata, K., Andrews, S. R. and Kelsey, G. (2011). Dynamic CpG island methylation landscape in oocytes and preimplantation embryos. *Nat. Genet.* **43**, 811-814.
- Spencer, S. L., Cappell, S. D., Tsai, F.-C., Overton, K. W., Wang, C. L. and Meyer, T. (2013). The proliferation-quiescence decision is controlled by a bifurcation in CDK2 activity at mitotic exit. *Cell* **155**, 369-383.
- Suetake, I., Shinozaki, F., Miyagawa, J., Takeshima, H. and Tajima, S. (2004). DNMT3L stimulates the DNA methylation activity of Dnmt3a and Dnmt3b through a direct interaction. *J. Biol. Chem.* **279**, 27816-27823.
- Sun, H., Wu, J., Wickramasinghe, P., Pal, S., Gupta, R., Bhattacharyya, A., Agosto-Perez, F. J., Showe, L. C., Huang, T. H.-M. and Davuluri, R. V. (2011). Genome-wide mapping of RNA Pol-II promoter usage in mouse tissues by ChIP-seq. *Nucleic Acids Res.* **39**, 190-201.
- Suzuki, H., Ahn, H. W., Chu, T., Bowden, W., Gassei, K., Orwig, K. and Rajkovic, A. (2012). SOHLH1 and SOHLH2 coordinate spermatogonial differentiation. *Dev. Biol.* **361**, 301-312.
- Van Emburgh, B. O. and Robertson, K. D. (2011). Modulation of Dnmt3b function in vitro by interactions with Dnmt3L, Dnmt3a and Dnmt3b splice variants. *Nucleic Acids Res.* **39**, 4984-5002.
- Vazquez, F., Ramaswamy, S., Nakamura, N. and Sellers, W. R. (2000). Phosphorylation of the PTEN tail regulates protein stability and function. *Mol. Cell. Biol.* **20**, 5010-5018.
- Vazquez, F., Grossman, S. R., Takahashi, Y., Rokas, M. V., Nakamura, N. and Sellers, W. R. (2001). Phosphorylation of the PTEN tail acts as an inhibitory switch by preventing its recruitment into a protein complex. *J. Biol. Chem.* **276**, 48627-48630.
- Webster, K. E., O'Bryan, M. K., Fletcher, S., Crewther, P. E., Aapola, U., Craig, J., Harrison, D. K., Aung, H., Phutikanit, N., Lyle, R. et al. (2005). Meiotic and epigenetic defects in Dnmt3L-knockout mouse spermatogenesis. *Proc. Natl. Acad. Sci. U.S.A.* **102**, 4068-4073.
- Wienholz, B. L., Kareta, M. S., Moarefi, A. H., Gordon, C. A., Ginno, P. A. and Chédin, F. (2010). DNMT3L modulates significant and distinct flanking sequence preference for DNA methylation by DNMT3A and DNMT3B in vivo. *PLoS Genet.* **6**, e1001106.
- Yang, J., Chai, L., Fowles, T. C., Alipio, Z., Xu, D., Fink, L. M., Ward, D. C. and Ma, Y. (2008a). Genome-wide analysis reveals Sall4 to be a major regulator of pluripotency in murine-embryonic stem cells. *Proc. Natl. Acad. Sci. U.S.A.* **105**, 19756-19761.
- Yang, J., Chai, L., Gao, C., Fowles, T. C., Alipio, Z., Dang, H. E., Xu, D., Fink, L. M., Ward, D. C. and Ma, Y. (2008b). SALL4 is a key regulator of survival and apoptosis in human leukemic cells. *Blood* **112**, 805-813.
- Yang, J., Aguila, J. R., Alipio, Z., Lai, R., Fink, L. M. and Ma, Y. (2011). Enhanced self-renewal of hematopoietic stem/progenitor cells mediated by the stem cell gene Sall4. *J. Hematol. Oncol.* **4**, 38.
- Yang, F., Yao, Y., Jiang, Y., Lu, L., Ma, Y. and Dai, W. (2012a). Sumoylation is important for stability, subcellular localization, and transcriptional activity of SALL4, an essential stem cell transcription factor. *J. Biol. Chem.* **287**, 38600-38608.
- Yang, J., Corsello, T. R. and Ma, Y. (2012b). Stem cell gene SALL4 suppresses transcription through recruitment of DNA methyltransferases. *J. Biol. Chem.* **287**, 1996-2005.
- Yeyati, P. L., Shaknovich, R., Boterashvili, S., Li, J., Ball, H. J., Waxman, S., Nason-Burchenal, K., Dmitrovsky, E., Zelent, A. and Licht, J. D. (1999). Leukemia translocation protein PLZF inhibits cell growth and expression of cyclin A. *Oncogene* **18**, 925-934.
- Zamudio, N. M., Scott, H. S., Wolski, K., Lo, C.-Y., Law, C., Leong, D., Kinkel, S. A., Chong, S., Jolley, D., Smyth, G. K. et al. (2011). DNMT3L is a regulator of X chromosome compaction and Post-Meiotic gene transcription. *PLoS ONE* **6**, e18276.
- Zhang, J., Tam, W.-L., Tong, G. Q., Wu, Q., Chan, H.-Y., Soh, B.-S., Lou, Y., Yang, J., Ma, Y., Chai, L. et al. (2006). Sall4 modulates embryonic stem cell pluripotency and early embryonic development by the transcriptional regulation of Pou5f1. *Nat. Cell Biol.* **8**, 1114-1123.